Electrochemical Transducers – A New Approach to Ultrasound Sensor Design

Atif Shamsi[a], Sang-Eun Bae[a,*], Goran Majkic[b] and Stanko R. Brankovic[a,*,†]

*[a] Department of Electrical and Computer Engineering
and Center for Nanomagnetic Systems
[b]Department of Mechanical Engineering and
Texas Center for Superconductivity,
University of Houston, TX 77204-4005[a] (-4006[b])*

Abstract

We present a study investigating the electrochemical interface as a capacitive transducer for ultrasound sensor applications. The concept is demonstrated using a nanoporous Au layer as a sensing electrode. The sensing electrode was produced by dealloying of the $Ag_{0.8}Au_{0.2}$ bulk electrode yielding an Au layer with extremely high surface/volume ratio. This electrode configuration was tested against the state of the art piezoelectric sensor subjected to electrolyte excitation with ultrasound waves having 40 kHz frequency and 4000 Pa amplitude. Our results demonstrate that nanoporous Au layer can be used as a capacitive transducer for sensing dynamic changes of pressure in electrolytes (ultrasound sensing). The sensitivity of this electrode can be readily adjusted by increasing the thickness of the dealloyed electrode layer. The transducer equation is developed and its practical relevance is discussed for electrochemical ultrasound sensor design.

---

* The Electrochemical Society Active Member
† Stanko.Brankovic@ mail.uh.edu

Introduction

The design of inexpensive but sensitive ultrasound sensors is in demand in many fields of medical research and diagnostics, military applications, as well as in many other areas of engineering and technology enterprise (1). Today, the typical ultrasound sensors and are based on magnetostrictive, piezoelectric or capacitive actuation as the transducing mechanism to convert the mechanical energy of ultrasound waves into a readable electrical signal. Usually, the nature of the application, together with the sensor cost, its reliability and sensitivity are the governing parameters in the choice of the utilized transducing mechanism and the corresponding sensor design.

The electrified (electrochemical) interface represents a natural gateway to a variety of physical and chemical phenomena. The occurrences of these phenomena are detected either as faradic (charge transfer) or non-faradic (double layer charging/discharging) currents which can be used as a measurable sensing signal (2). Some time ago, *Yeager et al.*, (3,4) and *Kukoz et al.* (5) have demonstrated that electrified interfaces can also be used as an effective transducer for ultrasound in electrolytes *i.e.* "the electrochemical audio effect" (4,5). The origin of this effect has been described as a result of Double Layer Compression (DLC) and, early on, this phenomenon was recognized as potentially very useful for different analytical studies of the double layer structure and processes at the electrolyte/electrode interface. Surprisingly, these early efforts have received little research attention in subsequent years until more recent works by *Tankovsky et al.* (6,7,8,9) and *Lowe et al.* (10). The latter studies elucidated more details about the origin and practical applications of this phenomenon.

In this paper, a study investigating the potential for using an electrified interface as a capacitive transducer for ultrasound sensor design is presented. The sensing concept is demonstrated using a nanoporous Au layer as the sensing electrode. The nanoporous *Au* layer was produced by dealloying of the $Ag_{0.8}Au_{0.2}$ electrode yielding the *Au* structure with extremely high surface to volume ratio. The experimental results suggest that the dealloyed electrode layer (nanoporous *Au*) is an effective and low cost ultrasound sensor which sensitivity can be readily adjusted by increasing its thickness.

Experimental

The experimental setup for ultrasound measurements is presented in Figure 1A. The electrolyte in which the sensing electrode is immersed was 0.1 M $HClO_4$. The ultrasonic generator used for excitation of the electrolyte was the wall of an ultrasonic bath having 40 kHz fundamental frequency with displacement amplitude of ~10 nm. This amplitude corresponded to the change of pressure of ~ 4,000 Pa (11). The sensing electrode was produced by electrochemical dealloying of $Ag_{0.8}Au_{0.2}$ bulk electrode in solution containing 10^{-4} M Ag^+ + 0.1 M $HClO_4$. The starting $Ag_{0.8}Au_{0.2}$ alloy was produced using the Low Electro-Thermal Loss Spark Plasma Sintering (LETL-SPS) method (12). The sensing electrode was a cylindrical rod imbedded into epoxy resin holder with the exposed geometrical area of ≈ 1.8 cm^2. The representative outlook of the sensing electrode and the SEM image of its surface obtained after dealloying are shown in Figure

1B and 1C. During the measurements, the potential of the sensing electrode was kept constant. All potentials in this work are quoted *vs.* saturated calomel electrode (SCE). The current oscillations from the sensing electrode during experiments were measured using a PAR 263-A potentiostat. The current signal from the sensing electrode was converted directly into a voltage signal with 1:1 conversion ratio. Both signals, from the sensing electrode and from the state of the art piezoelectric sensor, were recorded simultaneously using a digital oscilloscope.
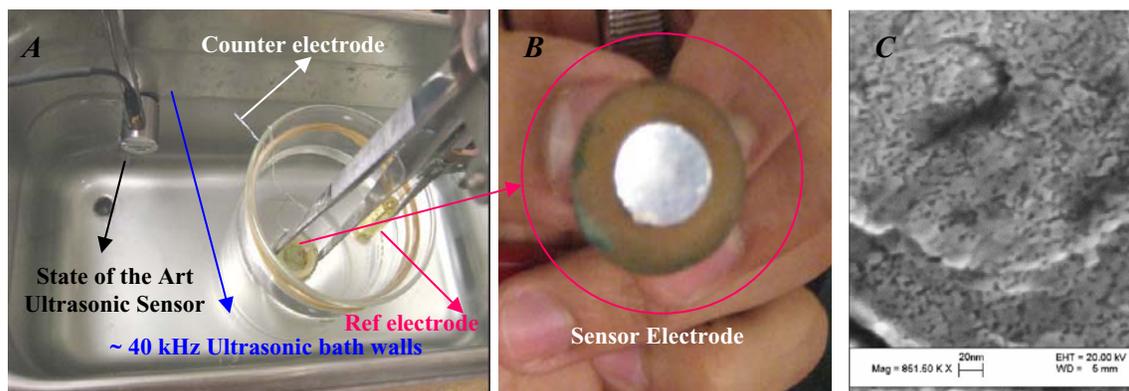

Figure 1. A) The experimental set up. The liquid filling the ultrasonic bath is water. The liquid in the glass beaker is the electrolyte. B) Sensing electrode, C) SEM image of the surface of the dealloyed layer – sensing layer (electrode).

Results and Discussion

Au Nanoporous Electrode

The dealloying of random binary alloys has been the subject of many fundamental and applied corrosion studies in the last several decades $(13, 14, 15, 16, 17, 18, 19)$. However, in recent years, the interest in this phenomenon has increased due to the potential applications of dealloyed structures in the different areas of nanomaterials synthesis, nanofabrication and electrocatalysis (20). The most accepted model in the literature describing the dealloying phenomenon is based on modified percolation theory (21) to define the thermodynamic and kinetic terms in the phenomenological expression for dealloying critical potential, E_C $(22,23)$. According to these considerations, the bulk dealloying of the less noble metal A at room temperature from the A_pB_{1-p} binary alloy occurs only for the alloys where the atomic fraction of the less noble component A is above its percolation threshold (for FCC metals, p > 0.6). If the applied potential to the electrode is more positive than the dealloying critical potential, selective bulk dissolution of the less noble component A from the A_pB_{1-p} alloy occurs and the remaining structure of the dealloyed electrode consist mostly of the more noble metal B. The typical linear sweep voltammetry for our bulk $Ag_{0.8}Au_{0.2}$ electrode in 0.1 M $HClO_4$ $+10^{-4}$ M Ag^+ is shown in Figure 2. In the same figure, the approximate value of the critical potential is indicated representing the onset of the bulk dissolution of Ag characterized by large increases in the current. The structure of the dealloyed electrode (mostly Au in our case) is characterized by very fine nanoporosity and high surface to volume ratio, as illustrated in Figure 1C.
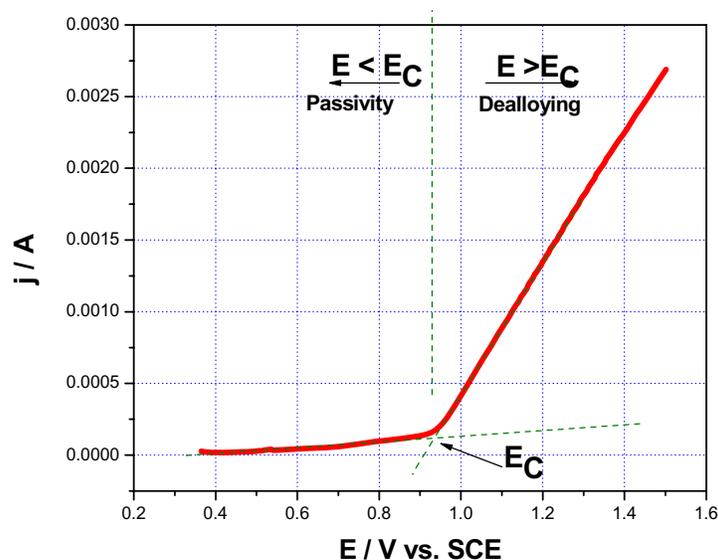
Figure 2. Linear sweep voltammetry for $Ag_{0.8}Au_{0.2}$ electrode in 0.1 M HClO$_4$ +10^{-4} M Ag$^+$ solution. Sweep rate 10 mV/s, the approximate value of $E_C \approx 0.95$ V.

In Figure 3, the increase in surface area of dealloyed $Ag_{0.8}Au_{0.2}$ electrode as a function of the dealloyed layer thickness is presented. The increase in area was estimated from the charge stripping measurements of the Pb *UPD* layer following the procedure reported previously by *Vukmirovic et al.* (13). As one can see, the increase of the area is a linear function with the slope of $\sim 1.2 \cdot 10^8$ m^{-1}. This means that the cube with 1 m^3 of the dealloyed electrode (Au nanoporous structure) would have the area of $1.2 \cdot 10^8$ m^2 which represents an increase by eight orders of magnitude relative to the initial geometrical area, A_0 (See the sketch in Figure 3). An electrode with such high surface/volume ratio represents a system where the electrochemical interface has a huge total double layer capacity and charge stored in electrical double layer.
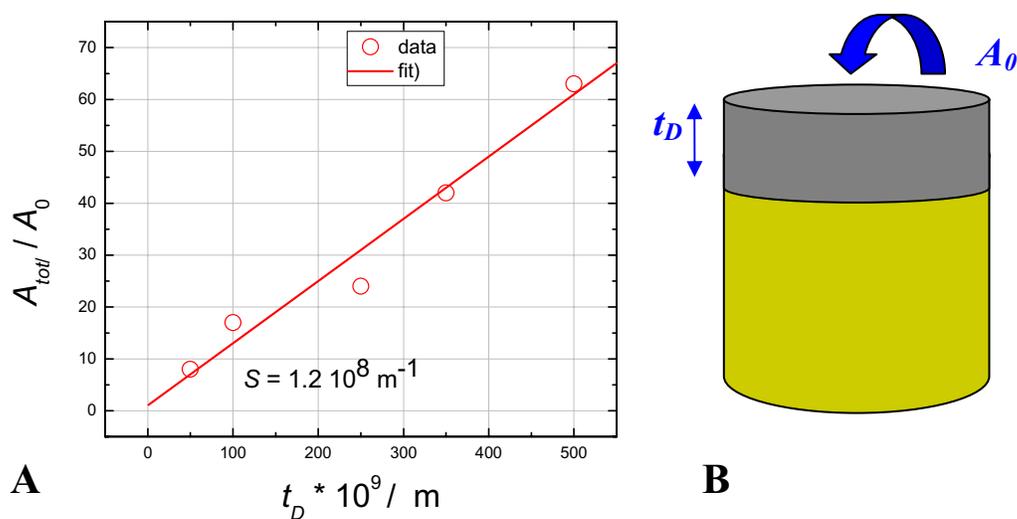

A **B**

Figure 3. A) Normalized area of the dealloyed layer as a function of its thickness. The slope of the linear fit is: $S = 1.2 \cdot 10^8$ m^{-1} . The total area can be estimated as $A = A_0 \cdot S \cdot t_h$ B) The schematics of the sensing electrode indicating the dealloyed layer on top of $Ag_{0.8}Au_{0.2}$ alloy.

Ultrasound Sensing

In Figure 4A, the recorded signals from our sensing electrode and the state of the art piezoelectric sensor (Figure 1) are shown for the ≈ 40 kHz ultrasound excitation of the 0.1 M HClO$_4$ electrolyte. The figure indicates that the ultrasound generator creates a periodic displacement/pressure wave of a broad frequency spectrum resembling a square wave profile with superimposed distortion. It is apparent that signals from both sensors follow the same wave profile with the same fundamental frequency and comparable amplitudes. A more quantitative comparison of these two signals is given in Figure 4B, showing their *Fourier* spectra. The higher terms in the spectra with frequencies above 1 MHz are excluded due to their negligible amplitude. It can be seen that the fundamental harmonic occurs at the same frequency of 39.8 kHz for both sensors, as expected from the specifications of the ultrasound generator used. The higher harmonics also coincide in terms of frequencies, while the ratio of their amplitudes to the fundamental amplitude shows reasonable agreement.
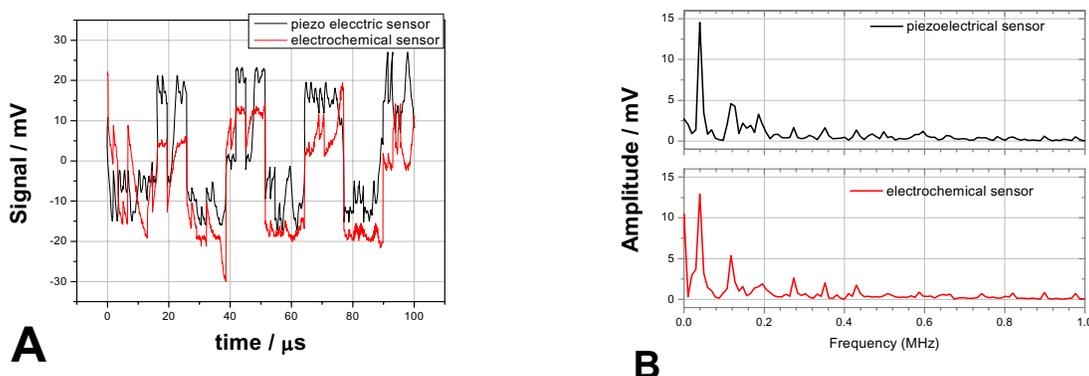

Figure 4. A) Signal transients from electrochemical and piezoelectric sensors B) *Fourier* transform of the signals shown in A. Red and black lines represent the signals from the electrochemical and piezoelectric sensors, respectively.

It is important to emphasize that in the present experimental setup, the piezoelectric sensor is in direct contact with the wall of the excitation source while the propagation of the ultrasound from the walls of the source (ultrasonic vessel) to the electrochemical cell is through fluids 1 (water) and 2 (0.1 M HClO$_4$), as well as through the glass wall of the electrochemical cell (Figure 1). The loss of ultrasound energy encountered during the passage through the two phase boundaries, 1) water/glass, and 2) glass/electrolyte, has to be evaluated in order to have proper insight into the actual differences in amplitudes of the pressure sensed by the electrochemical and piezoelectric sensors (Figure 1). To do that, we assume that both liquids and the glass are lossless transmission lines and we use an expression for the transmission coefficient for the glass plate submersed in liquid (24):

$$T = \frac{1}{1 + 0.25 \cdot \left(m - \frac{1}{m} \right)^2 \sin^2 \left(\frac{2\pi v}{c} \cdot d \right)} \tag{1}$$

Here, $m = 9.5$ is the ratio between acoustic impedances of glass ($Z_g = 14.1 \cdot 10^6$ kgm^{-2}s^{-1}) and water ($Z_w = 1.49 \cdot 10^6$ kgm^{-2}s^{-1}), c is the speed of sound in glass, d is the thickness of

the wall of the electrochemical cell and v is the frequency of the ultrasound. For $c = 5660$ m·s^{-1}, $d = 2 \cdot 10^{-3}$ m, and $v = 40$ kHz, the transmission coefficient T is evaluated to be $\approx$ 0.87. This means that the initial pressure amplitude, P_0, generated by our ultrasonic bath and sensed by the piezoelectric transducer is additionally reduced by factor of 0.93 (*viz.* $T = P^2/P_0^2 \Rightarrow P = T^{0.5}P_0$) before it reaches the electrochemical sensor. In fact, comparing the amplitudes between the main harmonics of the two signals shown in Figure 5B, the small difference can be noticed ($V_{EC} = 13 \cdot 10^{-3}$ V *vs.* $V_{PZ} = 14.6 \cdot 10^{-3}$ V). Nevertheless, as will be shown in the following section, the sensitivity of the sensing electrode can be readily scaled by controlling the thickness of the dealloyed layer, rendering an electrochemical sensor of higher sensitivity than the piezoelectric one. Thickness scaling can lead to significantly larger amplitudes of the electrochemical signal for the same experimental configuration as compared to the piezoelectric one. Evidence supporting this statement will be clear after the transducer equation is introduced followed by additional results.

Transducer equation

To develop a transducer equation for our sensor we start with a simplified view of the electrical double layer which can be described as parallel plate capacitor. For our electrolyte concentration this is a reasonable assumption, and the capacity of the double layer can be expressed using the *Helmholtz* model:

$$C_{dl} \approx C_H = \varepsilon_0 \varepsilon_r \frac{A}{x_0} \qquad (2)$$

Here, ε_0 and ε_r are the dielectric constant of vacuum and the relative dielectric constant of water in the double layer region, respectively (30 (25)), while A is the total area of the electrode surface in contact with the electrolyte and x_0 is the distance between the inner and outer *Helmholtz* planes. The change in double layer charge for a constant potential drop across the double layer, $\Delta\varphi$, ($\Delta\varphi = const$ for $E_{electrode} = const$) can be expressed as:

$$\partial Q = \Delta\varphi \cdot dC = \Delta\varphi \cdot \partial C_{dl} \qquad (3)$$

The corresponding current related to the change in charge of the double layer is then:

$$i = \frac{dQ}{dt} = \Delta\varphi \cdot \frac{\partial C_{dl}}{\partial t} \qquad (4)$$

From eq. (2), $\partial C_{dl}/\partial t$ can be expressed as:

$$\frac{\partial C_{dl}}{\partial t} \approx \varepsilon_0 \varepsilon_r \cdot A \frac{\partial \left(\frac{1}{x_0} \right)}{\partial t} = -\varepsilon_0 \varepsilon_r \cdot A \frac{1}{x_0^2} \frac{\partial x_0}{\partial t} \qquad (5)$$

The instant pressure change in the electrolyte results in the corresponding change of its volume. This relation can be described by:

$$\frac{\Delta V}{V} = -\frac{1}{K_{V,H_2O}} \cdot \Delta P \qquad (6)$$

Here, $K_{V,H2O}$ is the bulk modulus of water (2 GPa). According to the DLC model (10), at the interface, the relative change of the volume of the electrolyte is approximately equal to the relative change in the distance between the inner and outer *Helmholtz* planes and the equation (6) is transformed into:

$$\frac{\Delta x_0}{x_0} \approx -\frac{1}{K_{V,H2O}} \cdot \Delta P \tag{7}$$

For $\Delta x_0 \to \partial x_0$ and $\Delta P \to \partial P$ and after multiplying the above expression with $\partial t/\partial t$ the, equation (7) can be transformed into:

$$\frac{\partial x_0}{\partial t} \approx -\frac{x_0}{K_{V,H2O}} \cdot \frac{\partial P}{\partial t} \tag{8}$$

The substitution of eq.(8) into eq.(5) and then eq.(5) into eq.(4) yields the final expression for the double layer current related to the dynamic change of pressure at the electrode/electrolyte interface as:

$$i \approx \Delta\varphi \cdot \varepsilon_0 \varepsilon_r \cdot A \cdot \frac{1}{K_{V,H2O} \cdot x_0} \frac{\partial P}{\partial t} \tag{9}$$

From Figure 3A, the total area of the sensing electrode in contact with the solution can be expressed as $A = A_0 \cdot S \cdot t_D$, where S is the slope estimated from the linear fit of the experimental data, and t_D is the thickness of dealloyed layer. The ultrasound wave can be considered, without loss of generality, as a sinusoidal function of pressure in time, expressed as $P = P_0 \cdot sin(\omega t + \phi)$ (26). An arbitrary pressure excitation wave profile can then be expressed by an infinite or truncated series of *sin* or *cos* terms via *Fourier* harmonic analysis. For simplicity, we will consider only one harmonic in the transducer equation, in which case the final expression for our electrochemical sensor can be written as:

$$i \approx \Delta\varphi \cdot \varepsilon_0 \varepsilon_r \cdot A_0 \cdot S \cdot t_D \cdot P_0 \frac{2\pi \cdot v}{K_{V,H2O} \cdot x_0} \cos(2\pi \cdot v \cdot t + \phi) \tag{10}$$

Some of the terms in equation (10) can be easily evaluated. The potential drop across the double layer for the potential range away from *PZC* (which is our case, $E_{Au,PZC} = -0.1\ V$, $E_{electrode} = 0\ V$) is of the order of 1V. The distance between the inner and outer *Helmholtz* planes is approximately equal to the *Debye's* length in the electrolyte which can be accurately calculated. For symmetric 0.1 M electrolyte (our case) x_0 is $\approx 10^{-9}$ m. For $\varepsilon_0 = 8.854\ 10^{-12}$ F·m^{-1} and ε_r of water in the double layer being 30, and taking previously defined values of S, (Figure 3A) and $K_{V,H2O}$, the maximum current (amplitude) sensed by the electrochemical sensor is defined as:

$$i_0 \approx 0.1[C \cdot m^{-3} Pa^{-1}] \cdot A_0 t_D \cdot P_0 v \tag{11}$$

In our experiment, the thickness of the dealloyed layer was $\approx 4 \cdot 10^{-6}$ m, $A_0 = 1.8 \cdot 10^{-4}$ m^2, and the $P_0 \cdot v$ product was $1.6 \cdot 10^8$ Pa·s^{-1} which yields the amplitude of the sensing current of $i_{max} \approx 12 \cdot 10^{-3}$ A. As one can see in Figure 4B, the amplitude of the main harmonic from the signal coming from the electrochemical sensor is $\approx 13 \cdot 10^{-3}$ V = $13 \cdot 10^{-3}$ A which

is in a good agreement with calculated value from transducer equation. Analyzing eq.(11), it is obvious that the sensing electrode will show a higher sensitivity for ultrasounds with higher frequencies. Furthermore, it is important to notice that the current signal from the electrochemical sensor is directly proportional to the geometric volume of dealloyed layer ($A_0 \cdot t_D$). This means that if the effective dealloyed layer thickness is increased, an effective increase in signal magnitude should be expected. This is demonstrated in Figure 5. For the same ultrasound excitation of the electrolyte, but using a sensing electrode with six times thicker dealloyed layer ($t_D = 24 \cdot 10^{-6}$ m) the magnitude of the sensing signal has been increased for more than five times. This result clearly demonstrates that signal from our sensor is proportional to the electrode area and therefore its sensitivity can be easily increased to required level *i.e.* optimum level.
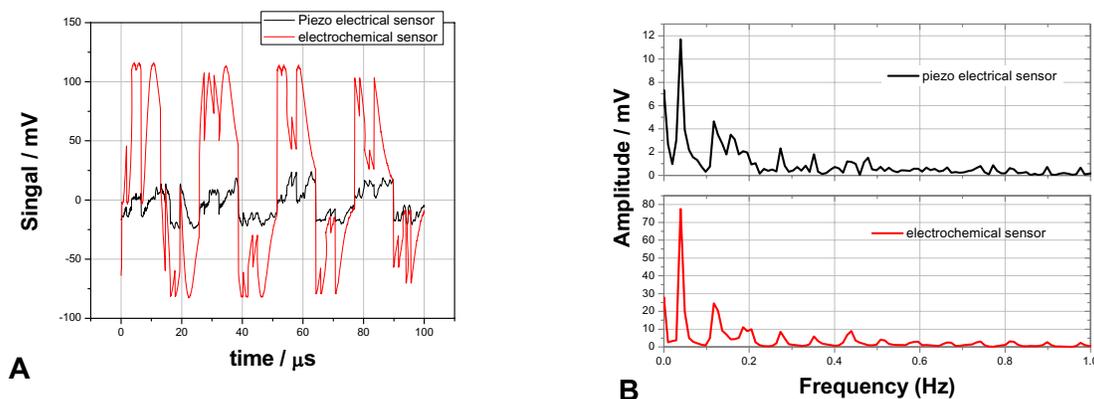

Figure 5. A) Signal transients from electrochemical and piezoelectric sensors B) *Fourier* transform of the signals in A. Red and black lines are signals from electrochemical and piezoelectric sensors, respectively.

Conclusions

In this paper the work demonstrating the electrochemical interface as an effective ultrasound transducer has been reported. A high surface to volume ratio electrode produced by dealloying was used as a model system to demonstrate the sensing concept. The transducing mechanism has been described as a result of the Double Layer Compression phenomenon. The transducer equation has been developed based on the *Helmholtz* model of the electrical double layer suggesting that the electrochemical interface is an ultrasound sensor which sensitivity is directly proportional to the frequency of the incident ultrasound wave. The surface area of the electrode has been demonstrated to be an adjustable design parameter that acts as a proportional amplifier of the sensing signal, thus making the electrochemical sensor a generic device with a potentially wide application range for ultrasound sensing in electrolytes.

Acknowledgment

References:

1. D. Ensminger, *Ultrasonics, Fundamentals, Technology, Application*, 2nd edition, Marcel Dekker, INC, NY (1988).
2. *Ultrathin Electrochemical Chemo-and Bio Sensors*, ed. V. M. Mirsky, Springer-Verlag, Berlin (2004).
3. F. Borsay, and E. Yeager, *J. Acoust. Soc. Am.*, **64,** 240 (1978).
4. E. Yeager, J. Bugosh, H. Dietrick, and F. Hovorka, *J. Acoust. Soc. Amer.*, **22,** 686 (1950)
5. F.I. Kukoz, and L.A. Kukoz, *Russ. J. Phys. Chem.*, **36**, 367 (1962).
6. N. Tankovsky, *J. Appl. Phys.* **75**, 1239 (1994).
7. N. Tankovsky, J. Burov, *J. Phys. Chem.* **98**, 10930 (1994).
8. N. S. Tankovsky, *Appl. Phys. Lett.*, **69**, 3327 (1996).
9. N. Tankovisky, *J. Appl. Phys.* **87**, 538 (2000).
10. A. R. Glauseer, P. A. Robertson, and C. R. Lowe, *Sensors and Actuators* B, **80**, 68 (2001).
11. G. L. Gooberman, *Ultrasonics-Theory and Application,* The English Universities Press LTD, London (1968). p 12.
12. G. Majkic, N. Chennoufi, Y.C. Chen, and K. Salama, *Metallurgical and Materials Transactions A*, 38, 2529 (2007).
13. M. B. Vukmirovic, N. Dimitrov, K. Sieradzki, *J. Electrochem. Soc.*, **149**, B428, (2002).
14. I. C. Oppenheim *et al*, *Science,* **254**, 687 (1991).
15. R. Li, and K. Sieradzki, *Phys. Rev. Lett.*, **68,** 1168 (1992).
16. K. Sieradzki, R.R. Corderman, K. Shukla and R. C. Newman, *Philosoph. Mag. A*, **59**, 713 (1989).
17. B. G. Ateya, G. Geh, A.H. Carim, H. W. Pickering, *J. Electrochem. Soc.*, **149,** B27 (2002).
18. H.W. Pickering, *Corrosion*, *Science*, **23**, 1107 (1983).
19. H. W. Pickering, C. Wagner, *J. Electrochem. Soc.*, **114**, 698 (1967).
20. J. Erlbacher, M.J. Aziz, A. Karma, N. Dimitrov, and K. Sieradzki, *Nature,* **410**, 6827 (2001).
21. D. Stauffer, in *Introduction to Percolation Theory*, p. 22, Taylor and Francis, London (1985).
22. K. Sieradzki, *J. Electrochem. Soc.*, **140**, 2868 (1993).
23. K. Sieradzki *et al*, *J. Electrochem. Soc.*, **149**, B 370 (2002).
24. G. L. Gooberman, *Ultrasonics-Theory and Application,* The English Universities Press LTD, London (1968). p 22.
25. W. Schmickler, *Interfacial Electrochemistry,* Oxford University Press, NY (1996) p.280.
26. T. D. Rossing and N. H. Fletcher, *Principles of Vibrations and Sound,* 2nd edition, Springer, NY (2004).